

# Lattice properties of strained GaAs, Si, and Ge using a modified bond-charge model

Resul Eryigit and Irving P. Herman

*Department of Applied Physics and Columbia Radiation Laboratory, Columbia University, New York, New York 10027*

(Received 17 August 1995)

A phenomenological lattice dynamics model based on the bond-charge model has been developed that describes how strain affects phonon frequencies and elastic constants in groups IV (homopolar) and III-V (heteropolar) semiconductor thin films and strained layers. A quasiharmonic approach is adopted, using force constants that depend linearly on strain. This model uses available experimental data and can predict the effect of arbitrary strains on nonpolar and polar semiconductor films. Using this model, the phonon dispersion relations are obtained for bulk and strained-layer heterostructures of Ge and GaAs on Si, and the mode Grüneisen parameters and the pressure dependence of second-order elastic constants are determined for bulk Si, Ge, and GaAs. Also, it is shown that analyzing the effect of strains on semiconductors leads to a better and more physical set of force constants for the bond-charge model for unstrained materials.

## I. INTRODUCTION

Studies of the lattice properties of strained semiconductors provide the information about lattice anharmonicity needed for a fundamental understanding of phonons and elastic constants and for the investigation of novel heterostructures.<sup>1-5</sup> These investigations include determining the dependence of zone-center optical phonon frequencies on hydrostatic pressure (isotropic strain) and the dependence of phonon frequencies on biaxial strain in strained-layer heterostructures, which are sometimes also under hydrostatic pressure.<sup>3</sup> Theoretical attempts to explain these findings can be broadly divided into two categories: those based on *ab initio* density-functional theory, using either a linear-response or frozen-phonon approach,<sup>6</sup> and those based on modifying phenomenological lattice-dynamical models. These lattice-dynamical models account for the presence of strain either by modifying the harmonic force constants, which is known as the quasiharmonic approximation, or by adding third- and higher-order anharmonic terms to the harmonic Hamiltonian. In a previous study, Sui and Herman<sup>3</sup> used both of these approaches to modify the Keating/valence-force-field (VFF) model to study, both analytically and numerically, the effect of arbitrary stress on phonon dispersion and elastic constants of group IV semiconductors and strained layers of these materials. This treatment can be applied only to nonpolar semiconductors. The current paper expands this study to polar semiconductors by modifying the Weber bond-charge model<sup>7-9</sup> (BCM) by using the quasiharmonic approximation. The modified bond-charge model is applied to GaAs, a polar semiconductor, and, for comparison purposes, to Si and Ge, nonpolar semiconductors.

The symmetry of a crystal can be altered by the presence of strains, and this symmetry change can lift phonon degeneracies. Also, phonon frequencies shift linearly with strain to first order. Such strains may result either from external stresses or from specific growth conditions or modifications of the materials. Built-in strains in epilayers and superlattices are produced by lattice mismatch or by compression following deposition at higher temperatures, due to the different

thermal expansion coefficients of the material layers involved. The measurement of phonon frequencies can be used as a diagnostic tool to determine such strains.<sup>10</sup> For example, Weinstein and co-workers<sup>11,12</sup> have considered how hydrostatic pressure tuning of lattice-mismatch-generated internal strain in two-component epitaxial films and multilayers (groups III-V/III-V and II-VI/III-V systems) affects Raman shifts. They used the microscopic  $p$ ,  $q$ , and  $r$  parameters to calculate the effect of tuning on the first-order Raman frequencies in systems grown along the (001) and (111) directions. Also, the folding of acoustic phonons and the confinement of optical phonons in superlattices can give rise to new  $k \approx 0$  zone-center phonons that are ir and/or Raman active, depending on the superperiodicity. These can also be affected by strain.

Several previous studies have attempted to model how strain affects phonon energies in partially ionic zinc-blende semiconductors. Cerdeira *et al.*<sup>4</sup> used the microscopic  $p$ ,  $q$ , and  $r$  parameters to account for the strain shift and splitting of the zone-center phonon frequencies. They evaluated these parameters by using Keating and valence-force-field models and assumed that the splitting between zone-center TO and LO modes in heteropolar semiconductors is independent of strain. Later, Hünemann *et al.*<sup>13</sup> employed effective charge deformation potentials to account for the different strain shift of these modes. Talwar and Vandevyver<sup>2</sup> used an 11-parameter rigid-ion model to study the effects of pressure on the vibrational properties of Ga-In pnictides. While their one-phonon and two-phonon densities of states, Debye temperatures, Grüneisen constants, and linear thermal expansion coefficients were all in reasonably good agreement with existing experimental data, their model predicted flatness of the lowest TA branches at ambient pressure but not at elevated pressures. This raised the question of whether the bending of the TA branch under compression was an artifact of the rigid-ion model or was due to the peculiarity of compound semiconductors.

Weinstein and Zallen<sup>1</sup> suggested use of the bond-charge model to study the pressure dependence of phonon dispersion relations. Mayer and Wehner<sup>14</sup> tried to extend the BCM to account for the strain-dependent phonon properties of Si

by including third-order anharmonic potentials. The model Grüneisen parameters they obtained were not in good agreement with available experimental values. They suggested that the problem was in the harmonic part of the potentials and then modified the BCM by including shell interactions similar to those in the shell model.<sup>15</sup> This model with eight harmonic and five anharmonic parameters produced reasonable agreement with experimental results. Very good agreement is obtained here by modifying the original BCM, with no added shells.

In this paper, the bond-charge model is reviewed in Sec. II A. This subsection also details how the BCM can be modified to include strain by modifying the force constants. In Sec. II B, the strain-modified force constants are determined by fitting the model to the experimentally available Grüneisen parameters. The mode Grüneisen parameters are determined along the  $\Gamma$ - $\Delta$ - $X$ - $K$ - $\Gamma$ - $L$ - $X$  directions in bulk Si, Ge, and GaAs. Section II C discusses how biaxial strain in the (001) and (111) planes affects phonon frequencies in GaAs and Ge epilayers on Si. This is followed by the treatment of the pressure dependence of phonon frequencies in strained Ge layers on Si(001) in Sec. II D. These results are discussed in Sec. III, and concluding remarks are presented in Sec. IV. A preliminary version of this paper was published as Ref. 16.

## II. MODEL

### A. The bond-charge model

#### 1. Ambient pressure

Several lattice-dynamical models have been designed to reproduce phonon dispersion curves, determined experimentally at ambient pressure, to the desired accuracy. One important characteristic of the phonon dispersion of diamond and zinc-blende semiconductors at ambient pressure that must be reproduced by the model is the very low frequency of TA branch phonons relative to LA phonons and the flatness of the TA branches away from the zone center. Strauch and Dorner<sup>17</sup> have compared the major phenomenological models on the basis of reproducing the phonon frequencies and eigenvectors and elastic constants of GaAs. The Weber bond-charge model<sup>7-9</sup> was found to be the model with the fewest adjustable parameters [four parameters for most diamond-structure materials (five for diamond) and six parameters for zinc-blende materials] to give the best fit to the experimental dispersion curves.

In the bond-charge model, adiabatically moving, pointlike bond charges (BC's) are introduced on the bonds to mimic the charge distribution of bonding electrons.<sup>8</sup> For homopolar semiconductors the BC's are in the middle of the bond, whereas for (heteropolar) III-V semiconductors they are nearer to the anions. The main BCM interactions are (a) the central potential between nearest-neighbor ions (ion-ion)  $\Phi_{i1-i2}$ , (b) the central potential between nearest-neighbor ions and BC's (ion-BC)  $\Phi_{i\nu-BC}$  ( $\nu=1, 2$ ), (c) the Keating bond-bond bending interaction (BC-BC)  $V_{bb}$ , and (d) the Coulomb interactions between all ion-ion, BC-BC, and ion-BC pairs  $V_{\text{Coulomb}}$ . These interactions are depicted in Fig. 1. Metal-like bonding is represented by the short-range central forces between ions ( $\Phi_{i1-i2}$ ) and covalent bonding is rep-

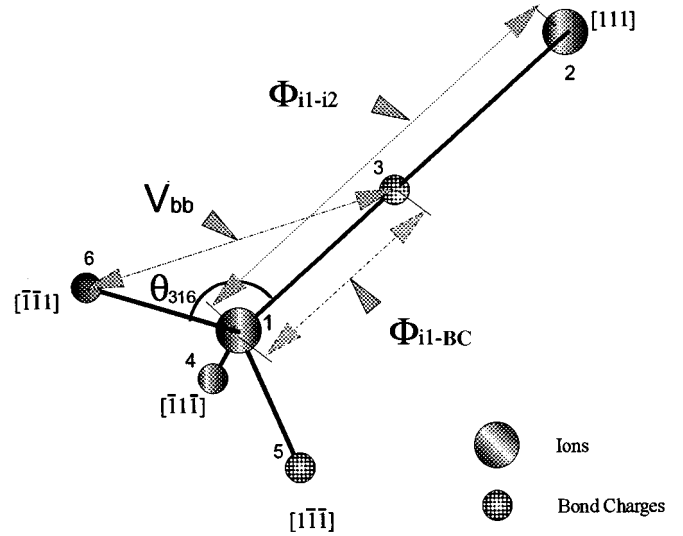


FIG. 1. Structure of the unit cell and the interactions in the bond-charge model.

resented by the Keating interactions between the BC's ( $V_{bb}$ ). For interaction (b) there are separate terms due to the interactions of the bond charges with cations and anions, and for interaction (c) there are different force constants associated with the BC-cation-BC and BC-anion-BC angles.

Bond charges of magnitude  $-Ze$  are located at  $r_1 = r_0(1+p)/2$  and  $r_2 = r_0(1-p)/2$ , where  $r_1$  and  $r_2$  are the respective distances to the cation (always labeled as 1) and anion (labeled as 2), respectively, and  $r_0$  is the bond length between nearest-neighbor ions. For homopolar (diamond) semiconductors  $p=0$  and for III-V (zinc-blende) semiconductors, including GaAs, it has been found that  $p=0.25$  at ambient pressure. Ions are assumed to carry the charge  $2Ze$ .

The total energy of the unit cell can be written using the above interactions:

$$\Phi_{\text{total}} = 4\Phi_{i1-i2}(r_0) + 4\Phi_{i1-BC}(r_1) + 4\Phi_{i2-BC}(r_2) + 6[V_{bb}^{(1)} + V_{bb}^{(2)}] + 6[\Psi_1(t_1) + \Psi_2(t_2)] - \alpha_M \frac{4Z^2 e^2}{\epsilon r_0}, \quad (1)$$

where  $\epsilon$  is the dielectric constant,  $\alpha_M$  is the Madelung constant, and  $t_1$  and  $t_2$  are the distances between any pair of bond charges adjacent to ion 1 and ion 2, respectively; the last term is the total Coulomb energy of the unit cell. This equation also includes an additional central force interaction ( $\Psi$ ) between bond charges, which has been found to improve the model.<sup>9</sup> It is defined by

$$\Psi'_1 = \Psi'_2 = 0 \quad \text{and} \quad \Psi''_1 = -\Psi''_2 = (\beta_2 - \beta_1)/8, \quad (2)$$

where  $\beta_\nu$  is defined below.

In the harmonic approximation, the equation of motion of the crystal is written as<sup>18</sup>

$$M_\kappa \ddot{u}_i(l\kappa) = - \frac{\partial \Phi_{\text{total}}}{\partial u_i(l\kappa)} = - \sum_{l'\kappa'} \varphi_{ij}(l\kappa; l'\kappa') u_j(l'\kappa'), \quad (3)$$

where  $l\kappa$  is the index for the  $\kappa$ th atom in the  $l$ th unit cell,  $M_\kappa$  is the mass of atom  $\kappa$ , and  $u_i(l\kappa)$  is the  $i$ th component ( $x, y$ , or  $z$ ) of the displacement of atom  $l\kappa$ .  $\varphi_{ij}(l\kappa; l'\kappa')$  is called the atomic force constant and is given by

$$\varphi_{ij}(l\kappa; l'\kappa') = \left. \frac{\partial^2 \Phi_{\text{total}}}{\partial u_i(l\kappa) \partial u_j(l'\kappa')} \right|_0, \quad (4)$$

where 0 implies that the derivatives are evaluated at the equilibrium point and  $\Phi_{\text{total}}$  is the total potential energy of the unit cell.

The explicit form of the Keating bond-bending interaction is

$$V_{bb}^{(\nu)}(\kappa; \kappa') = \frac{\beta_\nu}{8a_{0\nu}^2} [\mathbf{R}(\kappa\nu) \cdot \mathbf{R}(\kappa'\nu) + a_{0\nu}^2]_0^2, \quad (5)$$

$$\kappa, \kappa' = 3, 4, 5, 6,$$

where  $\nu=1$  or  $2$  depending on whether  $\kappa$  and  $\kappa'$  is adjacent to ion 1 or ion 2,  $\mathbf{R}(\kappa\nu)$  is the position vector of the BC with respect to the ion at the bond-angle vertex, and  $a_{0\nu}^2 = -\mathbf{R}(\kappa\nu) \cdot \mathbf{R}(\kappa'\nu)|_0$ .

The atomic force constant for each of the three central interactions ( $\Phi_{i1-i2}$ ,  $\Phi_{i1-BC}$ , and  $\Phi_{i2-BC}$ ) can be expressed as<sup>18</sup>

$$\varphi_{ij}^{\text{cent}}(l\kappa; l'\kappa') = \left\{ \frac{r_i r_j}{r^2} \left[ \Phi'' - \frac{1}{r} \Phi' \right] + \frac{\delta_{ij}}{r} \Phi' \right\} \Bigg|_{\mathbf{r}=\mathbf{x}(l\kappa)-\mathbf{x}(l'\kappa')}, \quad (6)$$

where  $\mathbf{x}(l\kappa)$  is the position vector of the particle  $\kappa$  in the  $l$ th unit cell.

The atomic force constant from the Keating-type interaction (c), differentiated with respect to bond charges only, is

$$\varphi_{ij}^K(l\kappa; l'\kappa') = \frac{\beta_\nu}{4a_{0\nu}^2} R_i(\kappa'\nu) R_j(\kappa\nu), \quad \kappa, \kappa' = 3, 4, 5, 6, \quad (7)$$

while that differentiated with respect to bond charges and ions is

$$\varphi_{ij}^K(l\kappa; l'\kappa') = \frac{\beta_\nu}{4a_{0\nu}^2} \sum_{\tau=3}^6 R_j(\tau\nu) [R_i(\kappa'\nu) + R_i(\tau\nu)], \quad (8)$$

$$\kappa = 1, 2 \quad \text{and} \quad \kappa' = 3, 4, 5, 6.$$

The values of  $\Phi'$  in Eq. (6) are fixed by the lattice stability constraint, which is determined by the equilibrium conditions

$$\left. \frac{\partial \Phi_{\text{total}}}{\partial r_0} \right|_{r_0=(r_0)_{\text{equilibrium}}} = 0, \quad (9a)$$

$$\left. \frac{\partial \Phi_{\text{total}}}{\partial p} \right|_{p=(p)_{\text{equilibrium}}} = 0. \quad (9b)$$

Using Eqs. (1) and (9a),

$$\Phi'_{i1-i2} = -\alpha_M \frac{Z^2 e^2}{2\epsilon r_0^2}. \quad (10)$$

Using Eqs. (1) and (9b), along with the auxiliary condition given by Rustagi and Weber,<sup>9</sup>

$$(1+p)\Phi'_{i1-BC} + (1-p)\Phi'_{i2-BC} = 0, \quad (11)$$

one finds

$$\frac{\Phi'_{i1-BC}}{r_1} = 2 \frac{1-p}{1+p} \frac{d\alpha_M}{dp} \frac{Z^2 e^2}{\epsilon r_0^3} \quad (12)$$

and

$$\frac{\Phi'_{i2-BC}}{r_2} = 2 \frac{1+p}{1-p} \frac{d\alpha_M}{dp} \frac{Z^2 e^2}{\epsilon r_0^3}. \quad (13)$$

So at ambient pressure the BC model has six free parameters:  $\Phi''_{i1-i2}$ ,  $\Phi''_{i1-BC}$ ,  $\Phi''_{i2-BC}$ ,  $\beta_1$ ,  $\beta_2$ , and  $\zeta = Z^2/\epsilon$ . For homopolar systems  $\Phi_{i1-BC} = \Phi_{i2-BC}$  and  $\beta_1 = \beta_2$ , and so there are only four free parameters.

The equation of motion, Eq. (3), is solved with a choice of displacement of the form

$$u_i(l\kappa) = u_i(\kappa) \exp[-i\omega t + i\mathbf{k} \cdot \mathbf{x}(l)] \quad (14)$$

which transforms Eq. (3) into

$$M_\kappa \omega^2(\mathbf{k}) u_i(\kappa) = \sum_{\kappa', j} D_{ij}(\kappa\kappa'; \mathbf{k}) u_j(\kappa'), \quad (15)$$

where  $D_{ij}(\kappa\kappa'; \mathbf{k})$  are the elements of the Fourier-transformed dynamical matrix, which are given by

$$D_{ij}(\kappa\kappa'; \mathbf{k}) = \sum_l \varphi_{ij}(0\kappa; l\kappa') \exp\{-i\mathbf{k} \cdot [\mathbf{x}(0\kappa) - \mathbf{x}(l\kappa')]\} + D_{ij}^C(\kappa\kappa'; \mathbf{k}), \quad (16)$$

where  $D_{ij}^C(\kappa\kappa'; \mathbf{k})$  is the Coulomb part of the dynamical matrix which is evaluated by using Ewald's method.<sup>18</sup>

Equation (15) is a set of 18 equations for the displacements of six particles. It can be reduced to a set of six equations for the displacements of the ions because the bond charges move adiabatically. This gives

$$\mathbf{D}^{\text{effective}} = \mathbf{D}^{\text{ion-ion}} - [\mathbf{D}^{\text{BC-ion}}]^* [\mathbf{D}^{\text{BC-BC}}]^{-1} \mathbf{D}^{\text{BC-ion}}, \quad (17)$$

where the  $\mathbf{D}$ 's are those parts of the dynamical matrix referenced by their superscripts and \* denotes Hermitian conjugation. The electron (bond-charge) interactions are now effectively included as ion-ion forces.

Vibrational frequencies and displacements are obtained from the eigenvalue equation

$$|D_{ij}^{\text{effective}}(\kappa\kappa'; \mathbf{k}) - M_\kappa \omega^2(\mathbf{k}) \delta_{ij} \delta_{\kappa\kappa'}| = 0, \quad (18)$$

where now  $\kappa$  and  $\kappa' = 1, 2$ . The second-order elastic constants are calculated with the long-waves method.<sup>18</sup> The values of the force constants used at ambient pressure are listed in Table I.

TABLE I. Harmonic force constants and their strain-modifier parameters. The first five rows have units of  $e^2/V$ , where  $V$  is the unit-cell volume (with data from Ref. 8 for Si and Ge and Ref. 9 for GaAs); the other rows are unitless.

	Si	Ge	GaAs <sup>a</sup>
Harmonic force constants			
$\Phi''_{i1-i2}$	18.63	19.83	18.48
$\Phi''_{i1-BC}$	19.41	17.13	7.05
$\Phi''_{i2-BC}$	19.41	17.13	48.15
$\beta_1$	8.60	8.40	5.36
$\beta_2$	8.60	8.40	8.24
$\zeta$	0.180	0.162	0.187
Strain-modifier parameters			
$m_{i1-i2}$	-12.70	-12.73	-12.77
$m_{i1-BC}$	12.19	12.27	-6.12
$m_{i2-BC}$	12.19	12.27	9.74
$m_{\beta_1}$	-2.75	-1.18	-4.97
$m_{\beta_2}$	-2.75	-1.18	-2.66
$l_{\beta_1}$	-3.18	-2.54	-3.63
$l_{\beta_2}$	-3.18	-2.54	2.51
$m_\zeta$	11.83	12.55	13.57

<sup>a</sup>Reference 9 gives linear combinations of these harmonic force constants.

## 2. Arbitrary strain

For a strained crystal, the harmonic approximation is still used and it is assumed that atoms in the deformed crystal experience harmonic oscillations about their new equilibrium positions. The effect of strain is incorporated by including changes in the elements of dynamical matrix due to the presence of the strain.

The change in the atomic force constants derived from central forces [Eq. (6)] due to strain is

$$\Delta[\varphi_{ij}^{\text{cent}}(l\kappa; l'\kappa')] = \Delta\left[\frac{r_i r_j}{r^2}\right] \left[\Phi'' - \frac{\Phi'}{r}\right] + \frac{r_i r_j}{r^2} \Delta[\Phi''] + \left[\delta_{ij} - \frac{r_i r_j}{r^2}\right] \Delta\left[\frac{\Phi'}{r}\right] \quad (19)$$

and for Keating-type interactions [Eq. (7)] it is

$$\Delta[\varphi_{ij}^K(l\kappa; l'\kappa')] = \beta_\nu \Delta\left[\frac{R_i(\nu\kappa')R_j(\nu\kappa)}{4a_{0\nu}^2}\right] + \frac{R_i(\nu\kappa')R_j(\nu\kappa)}{4a_{0\nu}^2} \Delta\beta_\nu. \quad (20)$$

The first terms in Eqs. (19) and (20) give a ‘‘lattice contribution’’ due to changes in the geometry due to strain, which are, respectively,

$$\frac{1}{r^2} \left[\Phi'' - \frac{\Phi'}{r}\right] \sum_\lambda \left[r_i \delta_{j\lambda} + r_j \delta_{i\lambda} - \frac{r_i r_j r_\lambda}{r^2}\right] \Delta r_\lambda \quad (21a)$$

where  $\Delta r$  is the strain-induced change in  $r$ , and

$$\beta_\nu \Delta\left[\frac{R_i(\nu\kappa')R_j(\nu\kappa)}{4a_{0\nu}^2}\right]. \quad (21b)$$

In the second and third terms of Eq. (19) and the second term of Eq. (20), the changes in the first and second potential derivatives and the Keating  $\beta_\nu$  are taken in the *quasiharmonic approximation*. The central ion-ion and ion-BC interaction parameters are scaled with the change in the distance between the two ‘‘particles’’ (i.e., ions or BC’s), while the Keating bond-bending parameters are scaled with the change in the distance between BC’s and the change in the angle between the bond charges. Consequently,

$$\Delta\Phi''_{i1-i2} = \Phi''_{i1-i2} \left[m_{i1-i2} \frac{\Delta r_0}{r_0}\right], \quad (22a)$$

$$\Delta\Phi''_{i\nu-BC} = \Phi''_{i\nu-BC} \left[m_{i\nu-BC} \frac{\Delta r_\nu}{r_\nu}\right], \quad \nu=1,2, \quad (22b)$$

$$\Delta\beta_\nu(\kappa, \kappa') = \beta_\nu \left[m_{\beta_\nu} \left(\frac{\Delta t_{\kappa\kappa'}}{t_{\kappa\kappa'}}\right) + l_{\beta_\nu} \frac{\Delta[\cos(\theta_{\kappa\nu\kappa'})]}{\cos(\theta_{\kappa\nu\kappa'}^0)}\right], \quad \nu=1,2, \quad (22c)$$

where  $\Delta r_0$  is the change in the ion-ion distance,  $\Delta r_\nu$  is the change in the distance between ion  $\nu$  and the bond charge,  $t_{\kappa\kappa'}$  is the distance between the bond charges  $\kappa$  and  $\kappa'$ , and  $\theta_{\kappa\nu\kappa'}^0$  is the equilibrium bond angle (no strain) between bond charges  $\kappa$  and  $\kappa'$  around the ion  $\nu$ . Equations (10), (12), and (13) for  $\Phi'$  still apply at the new strained equilibrium position.

Only either the magnitude or position of the bond charge is assumed to change, according to

$$\Delta\zeta = \zeta \left[m_\zeta \frac{\Delta r}{r}\right], \quad (22d)$$

where  $\zeta$  is either  $Z^2/\epsilon$  or  $p$ , and  $r$  refers to the length of the bond on which that bond charge is located. The Coulomb

force constants are calculated for strained crystals by using Ewald's method, which includes any "lattice contribution."

For the most general case, there are a total of eight force-constant-modifier strain parameters ( $m$ 's and  $l$ 's) in Eq. (22). For homopolar systems, this reduces to five parameters.

For an arbitrary strain, the position vectors and bond angles change as

$$\Delta \mathbf{x}(l\kappa) = \mathbf{u}_\kappa = \boldsymbol{\varepsilon} \cdot \mathbf{x}(l\kappa) - a\xi[\varepsilon_{yz}, \varepsilon_{xz}, \varepsilon_{xy}]^T + \mathbf{u}_d, \quad (23)$$

$$\Delta(\cos\theta_{\kappa\nu\kappa'}) = \frac{1}{2a}[\mathbf{R}(\kappa\nu) \cdot \mathbf{u}_{\kappa'} + \mathbf{R}(\kappa'\nu) \cdot \mathbf{u}_\kappa], \quad (24)$$

where  $\mathbf{u}_d$  is the dynamic displacement,  $\boldsymbol{\varepsilon}$  is the symmetric strain tensor,  $\mathbf{x}$  is the bond vector,  $\xi$  is the internal strain parameter,  $a = a_L/4$  for ions and  $a_L/8$  for bond charges ( $a_L$  is the lattice constant), and  $T$  stands for transpose.

The dynamical matrix for the strained lattice is obtained from Eq. (16) by the replacements

$$\varphi_{ij}(0\kappa; l\kappa') \rightarrow \varphi_{ij}(0\kappa; l\kappa') + \Delta[\varphi_{ij}(0\kappa; l\kappa')],$$

and

$$D_{ij}^C \rightarrow D_{ij}^C|_{\text{strained}} \quad (25)$$

where  $\Delta[\varphi_{ij}(0\kappa; l\kappa')]$  is calculated from Eqs. (19) and (20). Vibrational frequencies and displacements are obtained by using Eqs. (17) and (18) with the above replacements.

### B. Hydrostatic pressure

When the crystal is subjected to hydrostatic pressure, the strain is diagonal and is given by  $\varepsilon_h = -P/3B$ ;  $P$  is the applied pressure and  $B$  is the bulk modulus. The symmetry of the crystal is not lowered and consequently the bond angles do not change, so the  $l$  terms in Eq. (22c) vanish; bond lengths change by  $\Delta r = r_0 \varepsilon_h$ . The force constants are modified according to Eq. (22). The lattice contribution terms [Eqs. (21a) and (21b)] are zero. All of the  $m$  terms in Eq. (22) are determined here from the dependence of phonon frequencies on hydrostatic pressure at critical points. This dependence can be characterized by the mode Grüneisen parameter, which is defined as

$$\gamma_i = -d \ln \omega_i / d \ln V = -\Delta \omega_i / (3 \varepsilon_h \omega_i), \quad (26)$$

where  $V$  is the volume of the crystal and  $\omega_i$  is the frequency of the  $i$ th phonon mode.

The  $m$ 's are obtained by a nonlinear least-squares fit to experimentally available  $\gamma_i$ 's at the  $\Gamma$ ,  $X$ , and  $L$  points of the Brillouin zone (Table II). The mode Grüneisen parameters are calculated from Eq. (26) by taking the differences of the mode frequencies obtained from Eq. (18), by using the dynamical matrix [Eq. (25)], for ambient and small ( $\sim 0.01$ ) hydrostatic strains.

The harmonic force constants used for Si and Ge are from Ref. 8 and are listed in Table I, and the "input" mode Grüneisen parameters are those used in Ref. 3 and are listed in Table II. Several sets of (ambient-pressure) harmonic force constants were tested for Ge, each of which reproduces lattice properties at ambient pressure quite well. The quality of the fit of the modified BCM was found to be sensitive to the exact choice of harmonic force constants. The  $\chi^2$  for the

TABLE II. Mode Grüneisen parameters used in the nonlinear least-squares fit.

	Si	Ge	GaAs
$\gamma_{\text{LO}}(\Gamma)$	$0.98 \pm 0.06^a$	$1.14 \pm 0.02^c$	$1.23 \pm 0.02^d$
$\gamma_{\text{TO}}(\Gamma)$	$0.98 \pm 0.06^a$	$1.14 \pm 0.02^c$	$1.39 \pm 0.02^d$
$\gamma_{\text{LO}}(X)$	$1.03^b$	$1.17^b$	
$\gamma_{\text{TO}}(X)$	$1.50 \pm 0.2^a$	$1.49^b$	$1.73 \pm 0.07^e$
$\gamma_{\text{LA}}(X)$	$1.03^b$	$1.17^b$	
$\gamma_{\text{TA}}(X)$	$-1.4 \pm 0.3^a$	$-1.53 \pm 0.05^c$	$-1.62 \pm 0.05^e$
$\gamma_{\text{LO}}(L)$	$1.62^b$	$1.62^b$	
$\gamma_{\text{TO}}(L)$	$1.30 \pm 0.2^a$	$1.28^b$	$1.48 \pm 0.15^e$
$\gamma_{\text{LA}}(L)$	$0.45^b$	$0.55^b$	
$\gamma_{\text{TA}}(L)$	$-1.3 \pm 0.3^a$	$-1.4^b$	$-1.72 \pm 0.15^e$

<sup>a</sup>Reference 25 (experimental).

<sup>b</sup>Reference 3 (from *ab initio* calculation cited therein).

<sup>c</sup>Reference 26 (experimental).

<sup>d</sup>Reference 23 (experimental).

<sup>e</sup>Reference 20 (experimental).

quasiharmonic model fit of the Grüneisen parameters to the experimental data is small (3.1) for the set from Ref. 8 and larger (5.4) for that from Ref. 19. The quasiharmonic parameters for Si and Ge are listed in Table I. For Si and Ge,  $m_{i1-i2}$  and  $m_\beta$  are found to be negative, and  $m_{i1-BC}$  and  $m_\zeta$  are positive. This means that the ion-ion interactions get stronger with compression, whereas the ion-BC interactions get weaker. For Ge,  $m_{i1-i2}$ ,  $-m_{i1-BC}$ , and  $-m_\zeta$  are almost equal to each other ( $m_{i1-i2} \approx -12.7$ ); this is approximately true for Si. For both Si and Ge,  $m_\beta$  is very small, as is expected since the Keating bond-bending interaction is dependent on the bond angles and hydrostatic pressure does not change the angle between the bonds.

The harmonic force constants used for GaAs are from Ref. 9 and are listed in Table I, and the experimental mode Grüneisen parameters are listed in Table II. This choice of harmonic force constants is discussed in Sec. III. The calculated values of  $m$ 's for GaAs are given in Table I. These are the values obtained by taking the bond-charge position, and not its magnitude, as the fitting parameter. Fits were poorer when either only the bond charge was changed with strain or both the bond charge and position were changed. (For Si and Ge the bond-charge magnitude had to be changed.)  $m_{i1-i2}$  is very similar to that for Si and Ge ( $\approx -12.7$ ).  $m_\zeta \approx 13.6$  for the bond-charge position which suggests that bond charges are moving towards the center of the bond for isotropic strain. Consequently, it is reasonable that the strain parameters for ion-BC interactions for the cation and anions ( $m_{i1-BC}$  and  $m_{i2-BC}$ ) have opposite signs.

In Fig. 2, the dispersions in the Si, Ge, and GaAs mode Grüneisen parameters are plotted along the  $\Gamma$ - $\Delta$ - $X$ - $K$ - $\Gamma$ - $L$ - $X$  directions. Using these results, no substantial change in the shape of the TA branches with pressure is found, which is contrary to the results of Ref. 2.

The change in elastic constants is obtained by using the method of long waves<sup>18</sup> to obtain these constants for strained and unstrained structures, using the respective force constants, and then taking the difference. The pressure derivatives of the elastic constants are presented in Table III for Si, Ge, and GaAs. The calculated pressure derivatives of the

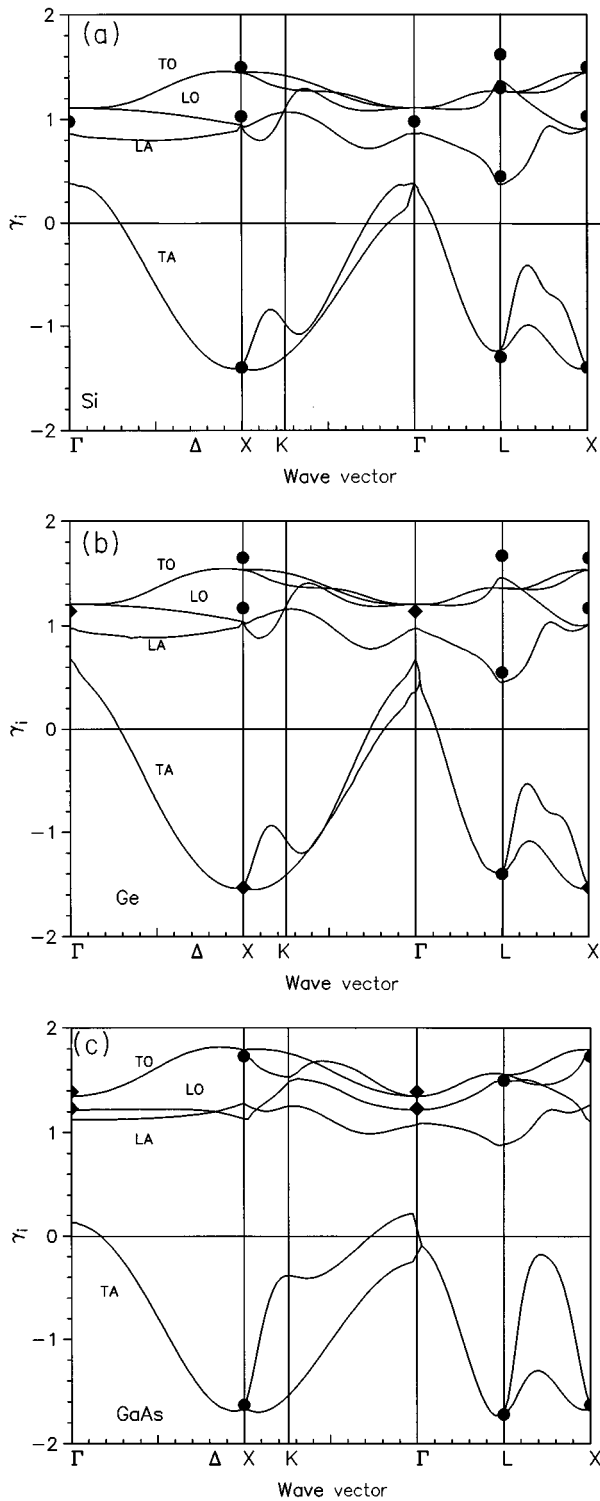


FIG. 2. Dispersion in mode Grüneisen parameters along the  $\Gamma$ - $\Delta$ - $X$ - $K$ - $\Gamma$ - $L$ - $X$  directions for (a) Si (circles are data from Ref. 3), (b) Ge (circles are data from Ref. 3, diamonds are data from Ref. 26), and (c) GaAs (circles are data from Ref. 20, diamonds are data from Ref. 23).

bulk modulus  $B$  for Si (4.91), Ge (5.21), and GaAs (5.24) are in reasonable agreement with the experimental values 4.24, 4.76, and 4.67,<sup>20</sup> respectively, as are the calculated pressure derivatives of the elastic constants  $C_{ij}$  for Si.<sup>21</sup> The general trends in the change of  $C_{11}$ ,  $C_{12}$ , and  $C_{44}$  with pressure are

TABLE III. Pressure derivatives of elastic constants for Si, Ge, and GaAs (unitless).

	Si	Ge	GaAs
$dC_{11}/dP$			
Calculated	4.9	5.2	5.3
Experimental	4.2 <sup>a</sup>		4.6 <sup>c</sup>
$dC_{12}/dP$			
Calculated	4.9	5.2	5.1
Experimental	4.2 <sup>a</sup>		4.6 <sup>c</sup>
$dC_{44}/dP$			
Calculated	2.1	2.9	2.4
Experimental	2.7 <sup>a</sup>		1.2 <sup>c</sup>
$dB/dP$			
Calculated	4.91	5.21	5.24
Experimental	4.24 <sup>b</sup>	4.76 <sup>b</sup>	4.67 <sup>b</sup>

<sup>a</sup>From Reference 21.

<sup>b</sup>From Reference 20.

<sup>c</sup>From Reference 2.

similar for Si, Ge, and GaAs.  $C_{11}$  and  $C_{12}$  change at nearly the same rate, which is much faster than that for  $C_{44}$ . The fit would be even better if the force-constant strain-modifier parameters had been determined by using both the experimental Grüneisen parameters and  $dC_{ij}/dP$ .

### C. Biaxial strains

Nonuniform strains modify the symmetry of the crystal and partially lift the degeneracy of some phonon modes, in addition to shifting the mode frequencies. In this model, biaxial strains in the (001) and (111) planes are used to determine the  $l$  parameters, which describe how the force constant of the Keating bond-bending interaction changes when strain changes bond angles [Eq. (22c)].

#### 1. Biaxial strain in the (001) plane

Biaxial strain in the (001) plane can arise during pseudomorphic growth of a thin film on a (001) substrate with a different lattice constant. The strain tensor can be decomposed into a hydrostatic part  $\epsilon_h = 2(1 - C_{12}/C_{11})\epsilon_{xx}/3$  and a shear part  $\epsilon_s = -(1 + 2C_{12}/C_{11})\epsilon_{xx}/3$ , where  $\epsilon_{xx} = (a_s - a_f)/a_f$ , and  $a_s$  and  $a_f$  are the lattice constants of the substrate and film, respectively. The  $C_{ij}$ 's are the (second-order) elastic constants of the film.

The hydrostatic component of the strain affects only the bond length, while the shear part changes only the bond angles. The distance between bond charges is affected by changes in both bond length and bond angle. Referring to Fig. 1, the fractional change in the cosine of the bond angle is  $4\epsilon_{xx}$  for the angles defined by the bond charge pairs 3-4, 3-5, 4-6, and 5-6, and it is  $-8\epsilon_{xx}$  for pairs 3-6 and 4-5. The distance between the bond charges in each pair changes by the same fraction. In homopolar materials, zone-center optical phonon frequencies split into a singlet and a doublet. In heteropolar materials, zone-center LO and TO modes split into a singlet and a doublet LO and a singlet and a doublet TO. In superlattices, in addition to these strain shifts there is

a frequency shift for optical phonons as a result of confinement.<sup>22</sup>

### 2. Biaxial strain in the (111) plane

When biaxial strain is in the (111) plane, in addition to the macroscopic strain an internal strain parameter  $\xi$  is needed to define uniquely the relative position of the atoms. This gives the relative displacements of the two face-centered-cubic lattices of the diamond structure.

The elements of the strain tensor are

$$\varepsilon_h = \frac{2C_{44}}{2C_{44} + C_{11} + 2C_{12}} \varepsilon_{\parallel}, \quad (27)$$

$$\varepsilon_o = \frac{C_{11} + 2C_{12}}{2C_{44} + C_{11} + 2C_{12}} \varepsilon_{\parallel}, \quad (28)$$

where  $\varepsilon_h$  and  $\varepsilon_o$  are the hydrostatic and shear components, and  $\varepsilon_{\parallel}$  is the in-plane lattice mismatch strain.

There are two different bond-length and bond-angle changes for this strain configuration. The change in the bond angle defined by the 3-4, 3-5, and 3-6 pairs is the negative of the change in other pairs. As with (001) strain, (111) strain splits each optical phonon at the  $\Gamma$  point into a singlet and a doublet.

### 3. Results

For Si and Ge, to obtain  $l_{\beta_1}$  the frequency splitting is needed at the  $\Gamma$  point when there is biaxial strain in either the (001) or (111) plane; the (001) splitting is used here to determine  $l_{\beta_1}$  and the (111) splitting is used to check this value. For GaAs, both strain configurations are needed to obtain  $l_{\beta_1}$  and  $l_{\beta_2}$ . The experimental data used are the same as those cited in Ref. 3 for Si and Ge, and determined in Ref. 23 for GaAs. The calculated  $l$  parameters are presented in Table I.

In Figs. 3 and 4, phonon frequency shifts for GaAs and Ge lattice matched to Si(001) and Si(111) (biaxial strain of  $\sim 0.04$  for both systems) are plotted using these strain-modified force constants. For this (001) biaxial strain configuration, the strain-induced shifts of the Ge LO and TO modes are seen to be very similar to those for the GaAs LO and TO modes, except the LO modes in Ge and GaAs differ greatly towards the zone boundary. The shift in the GaAs TO mode can become quite large ( $\sim 25 \text{ cm}^{-1}$ ). For the (111) strain configuration, the shifts and splittings of the corresponding modes in Ge and GaAs are qualitatively similar. For this configuration, the LO shift is significantly smaller than that for the TO mode for both Ge and GaAs ( $\sim 8 \text{ cm}^{-1}$  vs  $20 \text{ cm}^{-1}$ ).

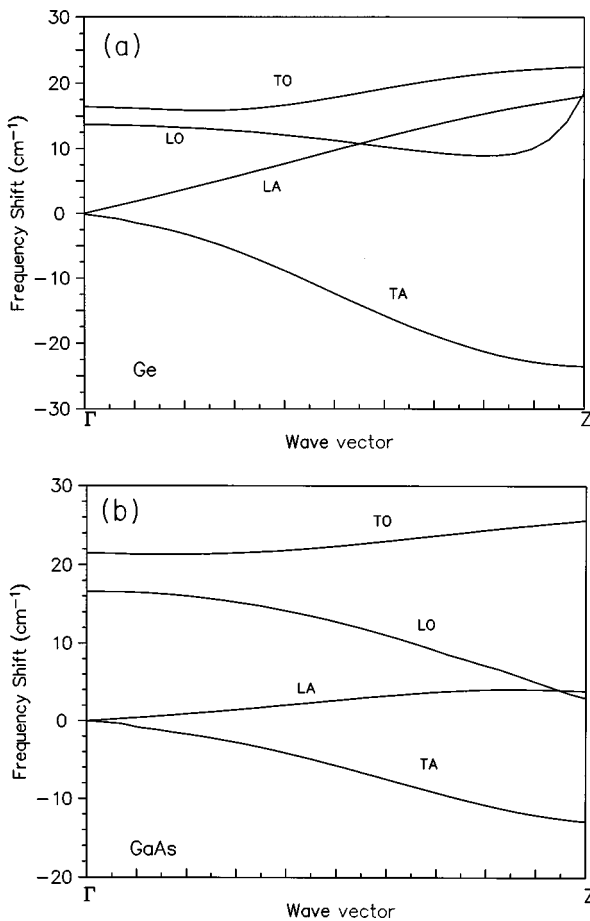


FIG. 3. Phonon frequency shifts  $\Delta\omega$  along the growth direction in (a) Ge and (b) GaAs commensurately grown on Si(001).

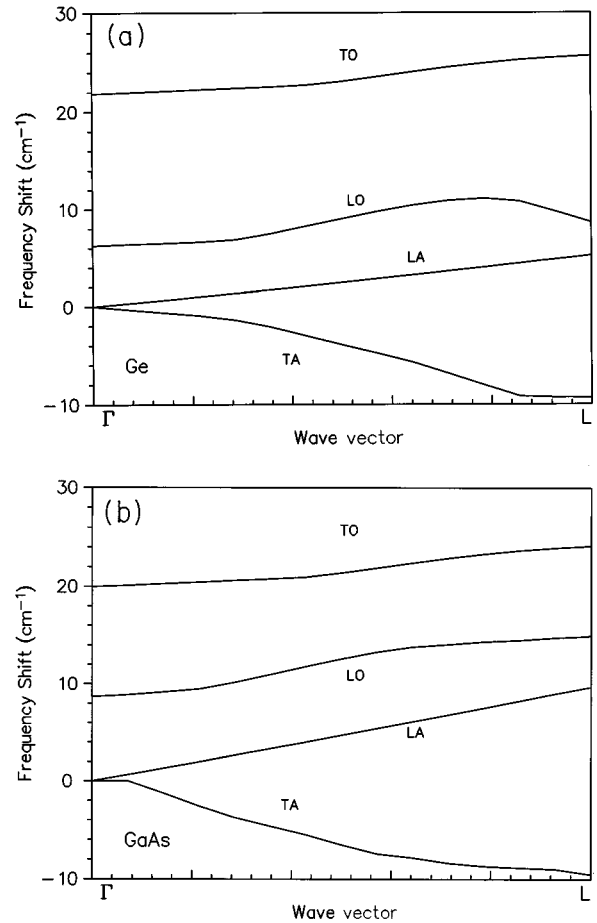


FIG. 4. Phonon frequency shifts  $\Delta\omega$  along the growth direction in (a) Ge and (b) GaAs commensurately grown on Si(111).

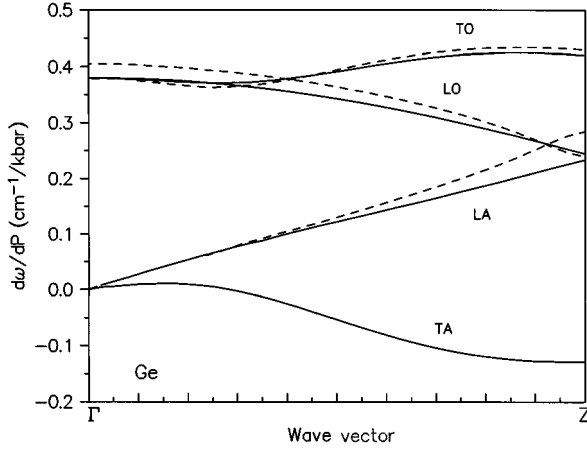


FIG. 5. Pressure derivatives of mode frequencies for Ge. Dashed lines are for Ge commensurately grown on Si(001) and solid lines are for bulk Ge.

#### D. Strained films under hydrostatic pressure

At ambient pressure, the lattice mismatch for Ge or GaAs grown on Si(001) is  $\sim 4\%$ . Under hydrostatic pressure, the hydrostatic part of the strain in the layer is

$$\varepsilon_{xx}^h = \varepsilon_{yy}^h = \varepsilon_{zz}^h = -\frac{P}{3B} + \frac{2}{3} \left[ 1 - \frac{C_{12}}{C_{11}} \right] \varepsilon_{xx}, \quad (29)$$

where  $\varepsilon_{xx}$  is the pressure-dependent lattice-mismatch strain, defined by

$$\varepsilon_{xx}(P) = \frac{a_s(P) - a_f(P)}{a_s(P)}. \quad (30)$$

$a_s(P)$  and  $a_f(P)$  are the pressure-dependent lattice constants for the substrate and film, respectively. Hydrostatic pressure tunes the built-in biaxial strain through Eq. (30), which to first order in  $P$  gives

$$\varepsilon_{xx}(P) = \varepsilon_{xx}(0) + \frac{a_f(0)}{a_s(0)} \left[ \frac{1}{3B_f} - \frac{1}{3B_s} \right] P, \quad (31)$$

where a 0 indicates the value at ambient pressure. For very small  $P$ , the pressure derivative of the phonon frequency is approximated by

$$\frac{d\omega}{dP} = \frac{\omega(\varepsilon^P, P) - \omega(\varepsilon^0, 0)}{P}, \quad (32)$$

where the superscripts  $P$  and 0 indicate values for applied hydrostatic pressure and for ambient conditions, respectively.  $d\omega/dP$  values for bulk and strained-layer films are compared in Fig. 5 for Ge pseudomorphically grown on Si(001) along the growth direction.

### III. DISCUSSION

Sui and Herman<sup>3</sup> used a modified Keating/VFF model to study the strain-dependent phonon properties of Si and Ge and heterostructures composed of these materials, both by using the quasiharmonic approximation used here and by adding cubic anharmonic terms to the interaction potential. The mode Grüneisen parameters obtained here for Si and Ge

are similar to those determined in Ref. 3. The modified BCM and Keating/VFF model have the same number of harmonic force constants and they perform similarly.

In addition to obtaining numerical results, Ref. 3 used the quasiharmonic approximation to derive analytic expressions that describe how strain changes phonon frequencies at the critical points in the Brillouin zone ( $\Gamma, X, L$ ), which could be fitted by experiment. In the current work, it is difficult to obtain analytic expressions because of the structure of the dynamical matrix [Eq. (17)] and the difficulty in inverting a  $12 \times 12$  matrix analytically. Though this matrix has a simpler structure for high-symmetry points and directions, it still cannot be inverted analytically for these special cases. [However, analytic expressions at the  $\Gamma$  point can be derived for homopolar (group IV) systems.]

One important difference between the findings of this work and those of Ref. 3 is in the change in the TA mode frequencies along the growth direction for Ge (Si) grown on Si (Ge) (001). Contrary to the results of Ref. 3 (see Figs. 5 and 6 in Ref. 3), it is found here that  $\Delta\omega(\text{TA})$  is negative (positive) along the growth direction for Ge on Si [Fig. 3(a)] (Si on Ge, not shown)—increasing in magnitude towards the zone boundary; this is also in agreement with the results of the *ab initio* calculations of Ref. 6. Taking into account the negative mode Grüneisen parameter for these branches and the fact that the traceless part of the biaxial strain does not affect the transverse mode frequencies much, it is expected that  $\Delta\omega(\text{TA})$  is negative (positive) for Ge on Si (Si on Ge) growth. This difference with Ref. 3 suggests that the interactions included in the Keating/VFF model may be insufficient and that the BCM interactions may be physically more sound. In the Keating/VFF model the flatness of the TA mode dispersion is determined by long-range interactions, while in the bond-charge model it is determined by a combination of ion-BC and BC-BC interactions.

Talwar and Vandevyver<sup>2</sup> modified the 11-parameter rigidity model to study the pressure dependence of several lattice properties, such as the thermal expansion coefficient, Grüneisen parameters, and Debye temperature, of group III-V materials by using 11 pressure parameters to scale the force constants. It is seen here that there is much better agreement in modeling the pressure dependence of phonon frequencies by modifying the bond-charge model. Moreover, fewer parameters are used with the modified BCM, 12 (six harmonic plus six strain modifiers) vs 22. Also, for GaAs the pressure bending of the TA branch near the  $X$  zone boundary is not found to be as strong as that found in Ref. 2. From the one-dimensional analysis by Weber,<sup>7</sup> one would expect that these branches become even flatter as pressure is increased due to a decrease in the ion-BC interaction and a slight increase in the BC-BC interaction.

The Grüneisen parameters calculated here are in good agreement with the available data from experiment and *ab initio* calculations. The model is poorest for  $\gamma_{\text{LO}}(L)$  for Si and Ge, mirroring the disagreement between the experimental and BCM calculated values for  $\omega_{\text{LO}}(L)$  at ambient pressure. There is not a similar correlation between the errors in the model phonon frequencies and Grüneisen parameters for other points in the Brillouin zone. For all three materials, the Grüneisen parameter fit is best for the TA branches, which is not surprising since at ambient pressure the BCM fits TA phonon dispersion particularly well.



As can be seen from Fig. 2, the fit for the mode Grüneisen parameters of GaAs is better than that of Si and Ge. In contrast, the fit for phonon dispersion at ambient pressure shows the opposite trend. The reason for this may be the consistency of the data points used in the fitting process. Since relatively few mode Grüneisen parameters have been measured for Ge, *ab initio*-determined parameters were used when an experimental value was not available, as was done in Ref. 3. For GaAs, all the Grüneisen parameters used have been obtained experimentally, though from different measurements (Table II). The GaAs fit was weighted by using the experimentally determined errors. However, for Ge the same error was assumed for all points because the error in the *ab initio*-obtained points is uncertain, and so the fit was unweighted. This assumption about the error, which is really an uncertain error, along with the possibility of large errors in these calculated points, could have caused the fit for Ge to be poorer than that for GaAs. Errors in the experimental data base (Table II) may be the reason why the Si fit is poorer than that for GaAs.

For all three semiconductors,  $m_{i1-i2}$  and  $m_{\beta}$  are found to be negative, and  $m_{i2-BC}$  and  $m_{\zeta}$  are positive. This means that the ion-ion interactions get stronger with compression, whereas the ion-BC interactions get weaker. Also, the ion-ion force constants ( $\Phi''_{i1-i2}$ ) and the associated strain parameter  $m_{i1-i2}$  are nearly equal for the three materials: Si (18.63; -12.70), Ge (19.83; -12.73), and GaAs (18.48; -12.77), respectively. The differences in the lattice-dynamical parameters for Ge and GaAs (Table I) illustrate the differences between a homopolar and a heteropolar semiconductor, since their reduced masses are nearly the same.

In the bond-charge model, the TA mode frequency at the X point for Ge is related to the force constants as  $\omega_{TA}^2(X) \propto [A_{\text{eff}}^{-1} + B_{\text{eff}}^{-1}]^{-1}$  where  $A_{\text{eff}}$  and  $B_{\text{eff}}$  are the effective ion-BC central and noncentral force constants, respectively. ( $A_{\text{eff}}$  is composed of  $\Phi''_{i-BC}$  and Coulombic terms, while  $B_{\text{eff}}$  is from the Coulombic terms.) The values obtained for the  $m$  parameters of Eq. (22) suggest a weakening in these effective interactions, which is consistent with the trend in the ion-ion force constants ( $\Phi''_{i1-i2}$ ) which increase under pressure. For GaAs, on the other hand, the bond charges move towards the center of the bond, which is accompanied by an increase (decrease) in the ion-BC force constants for interactions involving the cation (anion); this tends to make it similar to the homopolar (Ge) configuration. The “metalliclike” force constant (ion-ion) increases with a coefficient nearly equal to that for Ge. The negative zone-boundary TA Grüneisen parameters can also be discussed in terms of the one-dimensional analysis by Weber.<sup>7</sup> In this picture, the low frequency and flat structure of zone-boundary TA modes are associated with the ratio of the BC-BC force constant to the ion-BC force constant and adiabatic movement of bond charges. The higher the ratio the lower and flatter the curve. Under pressure the ion-BC interaction gets weaker (as suggested by the positive  $m_{i1-BC}$  coefficients for Si and Ge) and the BC-BC interaction gets stronger (a negative  $m_{\beta}$ ), which makes the ratio of these two force constants higher than that for the ambient-pressure case and lowers the frequencies. So a negative Grüneisen parameter would suggest a decoupling of bond charges from ions.

One important consideration in assessing this modified bond-charge model is whether it can be simplified, for example, by including fewer terms in the ambient-pressure model. Weber<sup>8</sup> has shown that for Ge there is good agreement between the experimental and calculated dispersion curves even when only nearest-neighbor Coulomb interactions are included. However, the Grüneisen parameters cannot be fitted to the modified BCM without these long-range Coulomb forces. Also, Ref. 19 has shown that the BCM can be fitted to group IV materials with only three parameters, by taking ion-ion and ion-BC central force constants equal, and that this fit is as good as that for the original four-parameter Weber model. However, the Grüneisen parameters cannot be fitted well to the quasiharmonic version of this three-parameter model. Furthermore, from the fitted Grüneisen parameters for Si and Ge, it is seen that the strain coefficient of these two force constants ( $m_{i1-i2}$  and  $m_{i1-BC}$ ) are almost equal in magnitude, but opposite in sign. This suggests that the three-parameter model is not physical.

Since it is well known that the parameter fits for phenomenological lattice-dynamics models are not unique,<sup>17,19,24</sup> a second consideration is whether the fit to the quasiharmonic model can be improved by a better choice of ambient-pressure parameters. This nonuniqueness is partly due to the limited data set used for the fit. Generally, phonon frequencies, and sometimes also elastic constants, are used. However, phonon eigenvectors are rarely used because experimental phonon displacements are not available for most materials. Clearly, a parameter set that is obtained with limited input data can lead to some false predictions. For example, the eigenvectors of LA and LO phonon modes at the X point in GaAs calculated using the BCM parameter sets from Refs. 9 and 17 do not agree with the experimental findings; these sets were derived from phonon frequencies and, for Ref. 9, also from elastic and piezoelectric constants. Another reason for nonunique parameter sets is the choice of the interactions between the atoms used in the model. If there is overlap of some of the interaction potentials chosen, there will be strong correlations between the model parameters, especially in models with a large number of adjustable parameters.

The parameters of the bond-charge model are highly correlated and several different sets of force constants give similar  $\chi^2$  in least-squares fits. For Ge, there are four-parameter sets given in Ref. 8 for the BCM with and without Coulomb interactions turned off beyond the first nearest neighbor (derived using elastic constants and phonon frequencies at the X, L,  $\Gamma$ , and K points) and the four-parameter fit in Ref. 19 (fitted to a much larger number of phonon frequencies, and without elastic constants). For GaAs, the two distinct sets obtained in Ref. 17 have nearly equal  $\chi^2$ , both of which give marginally better fits to the phonon dispersion than does the set from Ref. 9. Each of these different force-constant sets was used in the quasiharmonic BCM to determine which, if any, would lead to good fits with the inclusion of anharmonicity. As mentioned in Sec. II B, only the force constants from Ref. 8 (Ge) and Ref. 9 (GaAs) were able to fit both ambient-pressure and strained phonon frequencies. This demonstrates that analysis of the higher-order, strain dependence of phonon frequencies can help in determining a physically more meaningful set of force constants for the harmonic part of the interaction.

It is known that the BCM overestimates the magnitude of the (dynamic) effective charge.<sup>17</sup> It is not easy to isolate and, consequently, determine a relationship between one of the model interactions (parameters) and the effective charge. Bond charge is not directly related to the effective charge because they have different origins. The magnitude of the effective charge is mainly determined by the asymmetry in the ion-BC force constants and Coulomb interaction. Since the modified BCM uses the Grüneisen parameters at zone center for LO and TO phonons, it clearly reproduces the change in effective charge with pressure, within a factor that includes the dielectric constant and the effective mass, which also depend on pressure.

There are several ways to improve this quasiharmonic BCM model. One involves the use of eigendisplacements in determining the harmonic force constants. Another involves the assumption that all four bond charges in a unit cell are identical. Although this is a good approximation for ambient-pressure conditions, under arbitrary strain the change in the magnitude of some of the bond charges might be different from that of others. Yet another potential improvement involves relaxing the assumption of point bond charges, which

may not be a good approximation for strained semiconductors.

#### IV. CONCLUDING REMARKS

The bond-charge model has been modified to study the strain dependence of phonon frequencies of diamond- and zinc-blende-type semiconductors. Calculated mode Grüneisen parameters are in good agreement with experimental values. The pressure dependence of second-order elastic constants has been investigated and reasonable agreement was found with experimental values. It has been shown by using the quasiharmonic approximation that harmonic force constants of the model can be chosen more definitively by analyzing the strain dependence of phonon frequencies as well. This model can be applied to other group III-V semiconductors, as well as to II-VI semiconductors.

#### ACKNOWLEDGMENT

This work was supported by the Joint Services Electronics Program Contract No. DAAH04-94-G-0057.

- 
- <sup>1</sup>B. A. Weinstein and R. Zallen, in *Light Scattering in Solids IV*, edited by M. Cardona and G. Güntherodt (Springer-Verlag, New York, 1984).
- <sup>2</sup>D. N. Talwar and M. Vandevyver, *Phys. Rev. B* **41**, 12 129 (1990).
- <sup>3</sup>Z. Sui and I. P. Herman, *Phys. Rev. B* **48**, 17 938 (1993).
- <sup>4</sup>F. Cerderia, C. J. Buchenauer, F. H. Pollak, and M. Cardona, *Phys. Rev. B* **5**, 580 (1972).
- <sup>5</sup>E. Anastassakis, A. Cantarero, and M. Cardona, *Phys. Rev. B* **41**, 7529 (1991).
- <sup>6</sup>S. de Gironcoli, *Phys. Rev. B* **46**, 2412 (1992).
- <sup>7</sup>W. Weber, *Phys. Rev. Lett.* **33**, 371 (1974).
- <sup>8</sup>W. Weber, *Phys. Rev. B* **15**, 4789 (1977).
- <sup>9</sup>K. C. Rustagi and W. Weber, *Solid State Commun.* **18**, 673 (1976).
- <sup>10</sup>E. Anastassakis, in *Light Scattering in Semiconductor Structures and Superlattices*, edited by D. J. Lockwood and J. F. Young (Plenum, New York, 1991).
- <sup>11</sup>L. J. Lui, U. D. Venkateswaran, B. A. Weinstein, B. T. Jonker, and F. A. Chambers, in *Frontiers of High-Pressure Research*, edited by H. D. Hochheimer and R. D. Etters (Plenum, New York, 1991).
- <sup>12</sup>L. J. Lui, U. D. Venkateswaran, B. A. Weinstein, and F. A. Chambers, *Semicond. Sci. Technol.* **6**, 469 (1991).
- <sup>13</sup>M. Hünemann, W. Richter, J. Saalmüller, and E. Anastassakis, *Phys. Rev. B* **34**, 5381 (1986).
- <sup>14</sup>A. P. Mayer and R. K. Wehner, *Phys. Status Solidi B* **126**, 91 (1984).
- <sup>15</sup>M. T. Labrot, A. P. Mayer, and R. K. Wehner, in *Proceedings of the Xth Conference on Phonons, Heidelberg, 1989*, edited by S. Hunklinger (World Scientific, Singapore, 1990).
- <sup>16</sup>R. Eryigit, Z. Sui, and I. P. Herman, in *Thin Films: Stresses and Mechanical Properties V*, edited by S. P. Baker, P. Børgesen, P. H. Townsend, C. A. Ross, and C. A. Volkert, MRS Symposia Proceedings No. 356 (Materials Research Society, Pittsburgh, 1995), p. 295.
- <sup>17</sup>D. Strauch and B. Dorner, *J. Phys. Condens. Matter* **2**, 1457 (1990).
- <sup>18</sup>A. A. Maradudin, E. W. Montroll, G. H. Weiss, and I. P. Ipatova, in *Solid State Physics: Advances in Research and Applications*, edited by H. Ehrenreich, F. Seitz, and D. Turnbull (Academic, New York, 1971), Suppl. 3.
- <sup>19</sup>O. H. Nielsen, *Phys. Rev. B* **25**, 1225 (1982).
- <sup>20</sup>R. Trommer, H. Müller, M. Cardona, and P. Vogl, *Phys. Rev. B* **21**, 4870 (1980).
- <sup>21</sup>H. J. McSkimin and P. Andreatch, Jr., *J. Appl. Phys.* **35**, 2161 (1964).
- <sup>22</sup>B. Jusserand and M. Cardona, in *Light Scattering in Solids V*, edited by M. Cardona and G. Güntherodt (Springer-Verlag, Heidelberg, 1989).
- <sup>23</sup>P. Wickboldt, E. Anastassakis, R. Sauer, and M. Cardona, *Phys. Rev. B* **35**, 1362 (1987).
- <sup>24</sup>R. S. Leigh, B. Szigeti, and V. K. Tewary, *Proc. R. Soc. London Ser. A* **320**, 505 (1974).
- <sup>25</sup>B. A. Weinstein and G. J. Piermarini, *Phys. Rev. B* **12**, 1172 (1975).
- <sup>26</sup>D. Olego and M. Cardona, *Phys. Rev. B* **25**, 1151 (1982).